STEM CELLS

Heat-stable enterotoxin inhibits intestinal stem cell expansion to disrupt the intestinal integrity by downregulating the Wnt/β-catenin pathway

Jia-yi Zhou[1] | Deng-gui Huang[1] | Chun-qi Gao[1,2] | Hui-chao Yan[1] |
Shi-geng Zou[3] | Xiu-qi Wang[1]

[1]College of Animal Science, South China Agricultural University/Guangdong Laboratory for Lingnan Modern Agriculture/Guangdong Provincial Key Laboratory of Animal Nutrition Control/National Engineering Research Center for Breeding Swine Industry, Guangzhou, People's Republic of China

[2]Integrative Microbiology Research Centre, South China Agricultural University, Guangzhou, People's Republic of China

[3]Wen's Group Academy, Wen's Foodstuffs Group Co, Ltd, Xinxing, People's Republic of China

Correspondence
Xiu-qi Wang, College of Animal Science, South China Agricultural University/Guangdong Laboratory for Lingnan Modern Agriculture/Guangdong Provincial Key Laboratory of Animal Nutrition Control/National Engineering Research Center for Breeding Swine Industry, Guangzhou 510642, People's Republic of China.
Email: xqwang@scau.edu.cn

Abstract

Enterotoxigenic *Escherichia coli* causes severe infectious diarrhea with high morbidity and mortality in newborn and weanling pigs mainly through the production of heat-stable enterotoxins (STs). However, the precise regulatory mechanisms involved in ST-induced intestinal epithelium injury remain unclear. Consequently, we conducted the experiments in vivo (mice), ex vivo (mouse and porcine enteroids), and in vitro (MODE-K and IPEC-J2 cells) to explore the effect of STp (one type of STa) on the integrity of the intestinal epithelium. The results showed that acute STp exposure led to small intestinal edema, disrupted intestinal integrity, induced crypt cell expansion into spheroids, and downregulated Wnt/β-catenin activity in the mice. Following a similar trend, the enteroid-budding efficiency and the expression of Active β-catenin, β-catenin, Lgr5, PCNA, and KRT20 were significantly decreased after STp treatment, as determined ex vivo. In addition, STp inhibited cell proliferation, induced cell apoptosis, destroyed cell barriers, and reduced Wnt/β-catenin activity by downregulating its membrane receptor Frizzled7 (FZD7). In contrast, Wnt/β-catenin reactivation protected the IPEC-J2 cells from STp-induced injury. Taking these findings together, we conclude that STp inhibits intestinal stem cell expansion to disrupt the integrity of the intestinal mucosa through the downregulation of the Wnt/β-catenin signaling pathway.

KEYWORDS
enteroid, intestinal stem cell, spheroids, STp, Wnt/β-catenin signaling

1 | INTRODUCTION

Enterotoxigenic *Escherichia coli* (ETEC) is not only the main culprit of intestinal mucosal infection in piglets, inducing diarrhea, but also a major public health issue, causing a great number of illnesses and deaths worldwide, particularly in children in underdeveloped regions.[1-3] The pathogeny of ETEC-induced diarrhea is initiated when ETEC adheres to the intestinal cells, where they secrete adhesin and subsequently produce various enterotoxins, including heat-stable enterotoxins (STa and

STb) and a heat-labile enterotoxin (LT).[4] These enterotoxins induce the accumulation of cyclic guanosine monophosphate (cGMP) and cyclic adenosine monophosphate and cause a disturbance in the water and electrolytes balance through phosphorylation of cystic fibrosis transmembrane conductance regulator (CFTR) in the small intestine.[4]

Although the mechanisms of STa-induced intestinal cell secretions have been explained, advancements in therapeutics have been impeded by the lack of new targets that might promote regeneration after injury. A previous study found that STa increased luminal

volumes in a time- and concentration-dependent manner in mouse enteroids.[5] Interestingly, Lgr5^{+} stem cells expanded into a budding enteroid with morphology consistent with that of columnar epithelium and comparable with that of the crypt cells; in contrast, Bmi1^{+} stem cells acquired a spheroidal phenotype with simple and cuboidal epithelial characteristics, as examined ex vivo, and were partially rescued through supplementation with an agonist of Wnt/β-catenin signaling-R-spondin 1 (RSPO1).[6,7] Wnt/β-catenin participates in the orderly renewal of epithelium driven by intestinal stem cells (ISCs).[8] Its disturbance causes depletion of ISCs, which in turn leads to the loss of intestinal regeneration.[9-11] Accumulation of evidence showed that STa-induced CFTR is a potential regulator of β-catenin and suppresses enterocyte proliferation.[12,13] Even then, the mechanism by which STa regulates Wnt/β-catenin is still unclear.

Overall, the objective of this study was to investigate how STa affects the intestinal epithelial integrity in mice, enteroids, and intestinal epithelial cell lines. This work might provide a novel target for the repair of intestinal injury and a new strategy for preventing ETEC-induced intestinal injury for use in clinical and livestock production.

2 | MATERIALS AND METHODS

2.1 | Ethical statement

All animal procedures were performed in accordance with the Guidelines for the Care and Use of Laboratory Animals of South China Agricultural University (Guangzhou, Guangdong, China), and the experiments were approved by the Animal Ethics Committee of South China Agricultural University (Guangzhou, China).

2.2 | STp administration in mice

Ten 4-week-old male C57BL/6 mice were fasted for 12 hours before gavage administration of enterotoxin STp (E coli) trifluoroacetate salt (#H6248, Bachem, Bubendorf, Switzerland) solution (dissolved in phosphate-buffered saline [PBS]) at a concentration of 0 or 5.0 mg/kg body weight (BW) (five mice in each group). After 6 hours, the mice were euthanized with CO_2 inhalation, followed by cervical dislocation to ensure death.

2.3 | Intestinal crypt isolation and culture

The jejuna of the mice in each group were washed with ice-cold Dulbecco's phosphate-buffered saline (DPBS), after being opened longitudinally, and were incubated in DPBS containing 30 mM ethylenediaminetetraacetic acid disodium salt (Sigma-Aldrich, St. Louis, Missouri); then, fresh DPBS was added until high purity crypts were acquired. The crypts were suspended in Matrigel (BD Biosciences, San-Jose, California) and cultured in the complete culture medium, including approximately 45% advanced DMEM/F12, 45% conditioned medium with Wnt3a, R-spondin 3, and Noggin (WRN), 10% fetal bovine serum

Significance statement

The findings of this study demonstrate that STp inhibits intestinal stem cell (ISC) expansion to disrupt the integrity of intestinal mucosa through the downregulation of the Wnt/ß-catenin signaling pathway, and activation of Wnt/ß-catenin by its enhancer RSPO1 can reverse this process. The dysfunction of ISC is associated with occurrence and development of diarrhea and supports the notion that restoring Wnt-dependent ISCs is a promising therapeutic target for the intervention of Enterotoxigenic *Escherichia coli*.

(FBS), 100 U/mL penicillin, 100 μg/mL streptomycin, 1× N2 supplement (Invitrogen, Carlsbad, California), 1 mM N-acetylcysteine (Sigma-Aldrich), 50 ng/mL recombinant murine epidermal growth factor (PeproTech, Rocky Hill, New Jersey), 10 μM Y27632 (Stemgent, Cambridge, Massachusetts), 0.5 μM LY2157299 (Selleck, Houston, Texas), and 10 μM CHIR99021 (Stemgent). The enteroid-forming efficiency was calculated as the percentage of the number of colonies to the number of enteroids seeded, while the enteroid-budding efficiency was calculated as the ratio of the number of enteroid buds to the total number of enteroids.

2.4 | Enteroid treatment ex vivo

The mouse or porcine enteroids were broken by a syringe, suspended with fresh Matrigel at a ratio of 1:3, and then reapplied to 48-well plates (Jet Bio-Filtration Co., Ltd, Guangzhou, China). Enteroid debris was cultured in the complete medium containing different concentrations of STp. The culture conditions of the mouse enteroids were consistent with those of the mouse intestinal crypts, and the culture conditions of the porcine enteroids, which were developed from the jejunal crypts of 7-day-old crossbred piglets (Landrace × Yorkshire), as described previously.[14]

2.5 | Scanning electron microscopy evaluation

The jejunum samples were fixed with 2.5% glutaraldehyde overnight and then washed with PBS, treated with 1% osmium tetroxide in sodium cacodylate buffer for 1 hour, dehydrated with alcohol, and dried to the critical point (EM CPD300, Leica Microsystems, Wetzlar, Germany). After drying, the jejuna were glued to stubs using carbon tape and coated with gold. The jejuna were analyzed using an EVO MA 15 scanning electron microscope (Carl Zeiss AG, Jena, Germany).

2.6 | Immunohistochemistry

Sections of the jejunum or enteroids were incubated with primary antibodies (Table S1) overnight at 4°C. Secondary staining was

performed with fluorescein isothiocyanate isomer (FITC) or Cy3-conjugated antibodies (Jackson Laboratory, Jackson, Mississippi) at room temperature for 2 hours. The nuclei were stained with 4',6-diamidino-2-phenylindole (DAPI) for 5 minutes at room temperature. Pictures of the tissue sections were taken using a microscope (Ti2-U, Nikon, Tokyo, Japan).

2.7 | Diamine oxidase activity detection

The activity of diamine oxidase (DAO) was determined in the jejunum using a commercial DAO kit (#A088-1, Nanjing Jiancheng Bioengineering Institute, China). The procedure was performed according to the manufacturer's protocols. The color optical density (OD) absorbance was measured by a visible spectrophotometer at a wavelength of 340 nm.

2.8 | Cell culture and treatment

MODE-K, IPEC-J2, and CMT-93 cells were grown independently in the complete medium consisting of Dulbecco's modified Eagle's medium/F12 (DMEM/F12, Gibco, Waltham, Massachusetts) containing 10% FBS (Gibco) and 1% penicillin/streptomycin at 37°C in a 5% CO_2 incubator. All experiments were performed in triplicate using cells from passages 10 to 13. The cells were treated with STp at 24 hours after seeding.

2.9 | Construction of frizzled7 (FZD7)/β-catenin overexpression cell line

The cDNA of porcine *FZD7* and *β-catenin* were subcloned into the lentiviral vector (pCDH-CMV-MCS-EF1-CopGFP-T2A-puro System Biosciences, Mountain View, California). To produce recombinant lentiviruses, HEK293T cells were cotransfected with respective recombinant expression lentivectors in combination with triple plasmids system (pMD2.G, psPAX2, and pCDH-CMV-β-catenin-MCS-EF1-GFP-puro/pCDH-CMV-FZD7-MCS-EF1-GFP-puro). The control virus was produced using the cloning vector without insertion. After 48 hours, the virus supernatant was collected, purified, and concentrated, and then stored at −80°C.

Then, IPEC-J2 cells were seeded and cultured for 24 hours before being infected by control or recombinant *FZD7/β-catenin* lentiviruses. The positive cells were obtained through the puromycin screening. The cell samples were collected to detect the protein expression of FZD 7 or β-catenin.

2.10 | MTT assay

The viability of MODE-K, IPEC-J2, and CMT-93 cells was determined by MTT assays, as previously described by Li et al.[15] Cells from each group were cultured in 96-well plates (Jet Bio-Filtration Co., Ltd.) at 1.5×10^4 cells/mL in the medium. The cell numbers were quantified at 24, 48, 72, and 96 hours using the following protocol: After incubation with 20 μL of MTT solution (Sigma-Aldrich) for 4 hours, the resulting crystals were dissolved in dimethyl sulfoxide (Sigma-Aldrich), and the OD at a wavelength of 490 nm was evaluated using an ELISA reader (Bio-Rad, Hercules, California).

2.11 | Cell count assay

The MODE-K, IPEC-J2, and CMT-93 cells treated with/without STp were washed with PBS, detached with 0.25% trypsin (Sigma) for 3 to 5 minutes at 37°C, and then blocked with an equal volume of complete medium. The number of viable cells was determined using an automated cell counter (Countstar BioTec, Shanghai, China).

2.12 | EdU incorporation assay

The MODE-K, IPEC-J2, and CMT-93 cells treated with/without STp were fixed in 4% paraformaldehyde for 30 minutes. The EdU+ cell ratio was quantified by EdU staining using the Cell-Light EdU Apollo 567 DNA in vitro kit (RIBOBIO, Guangzhou, China) according to the manufacturer's instructions. Fluorescence images were obtained using a fluorescence microscope (Nikon, Melville, New York).

2.13 | Flow cytometry

The MODE-K and IPEC-J2 cells from each group were fixed with cell binding buffer and then mixed with 5 μL of annexin V-FITC for cell apoptosis analysis. After the addition of 5 μL of propidium iodide, the cells were incubated at room temperature for 10 minutes in the dark. The cell samples were then run on a Becton Dickinson FACScan (Beckman Coulter, Inc., Brea, California). The apoptosis percentage was assessed by the ratio of apoptosis cells to total cells.

2.14 | Paracellular permeability assay

An EVOM voltohmmeter (Millipore, Billerica, Massachusetts) with an STX-2 chopstick electrode was used to measure the trans-epithelial electrical resistance (TEER). The MODE-K, IPEC-J2, and CMT-93 cells were cultured in the medium for 4 days; and then treated with/without STp, and the TEER value was monitored at 0, 24, 48, 72, and 96 hours.

2.15 | Immunofluorescence

MODE-K, IPEC-J2, and CMT-93 cells were seeded into 48-well culture plates, fixed with 4% paraformaldehyde for 30 minutes, permeabilized with 0.3% Triton X-100 for 10 minutes, and blocked in a
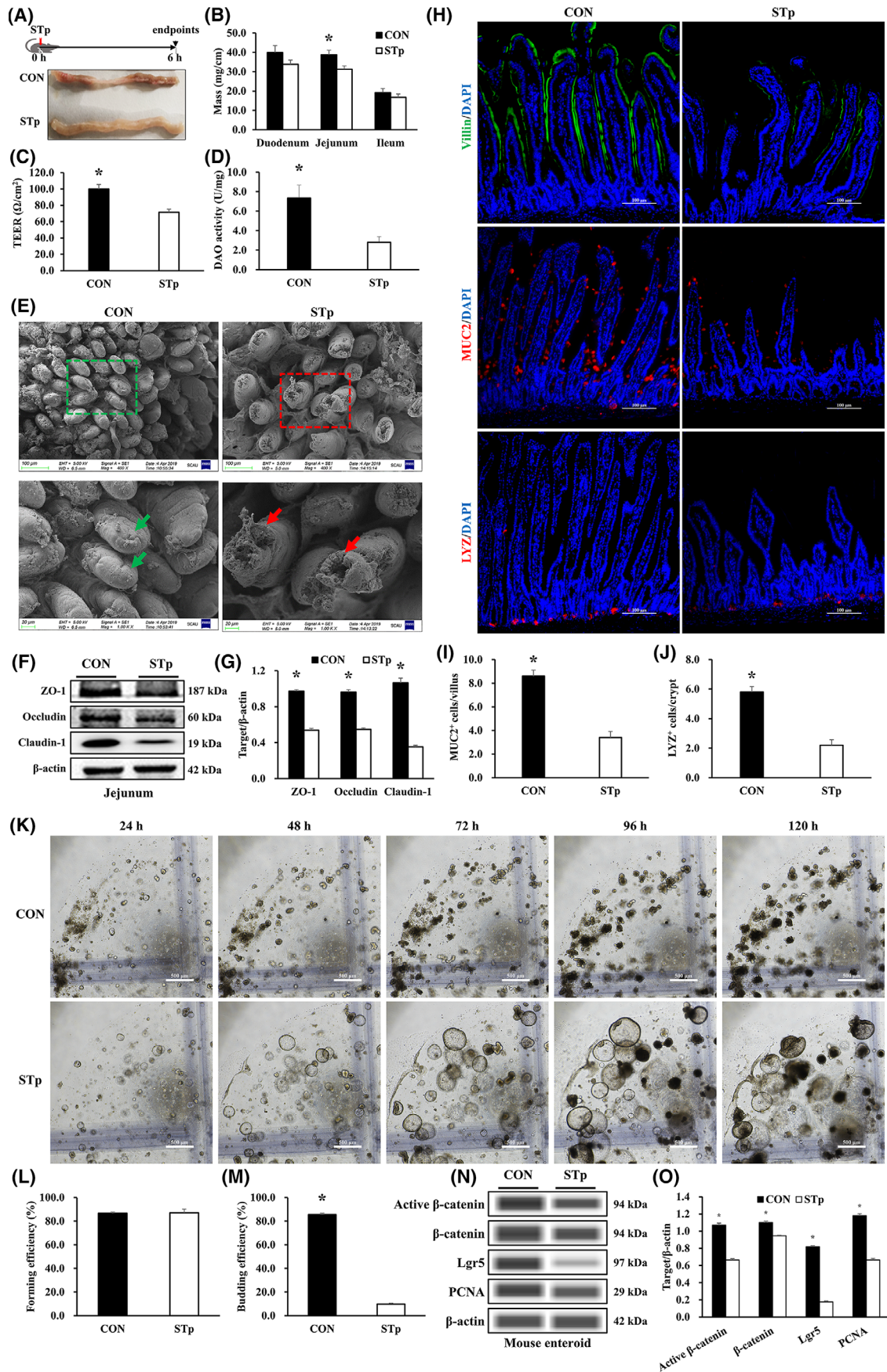
FIGURE 1 Legend on next page.

protein solution (Dako, Carpinteria, California) for 2 hours. The primary antibodies and secondary antibodies (Table S1) were incubated with the cells or enteroids. The nuclei were stained with DAPI for 5 minutes. Pictures were taken using a microscope (Ti2-U, Nikon, Tokyo, Japan). And the fluorescence signal intensity was analyzed by Image J software (National Institute of Health, Bethesda, Maryland).

2.16 | Isolation of total protein and Western blotting

The samples of the intestines, crypts, and cells from each group were collected for Western blotting analysis, as previously described.[16] These samples were lysed in radioimmunoprecipitation assay RIPA buffer and then centrifuged at 4°C for 30 minutes. The protein concentration of the supernatant was determined using a bicinchoninic acid protein assay reagent kit (Thermo Fisher Scientific, Rockford, Illinois). The proteins and color prestained protein marker (M222-10, GenStar, Beijing, China) were separated on 10% sodium dodecyl sulfate-polyacrylamide gel electrophoresis (SDS-PAGE) gels and then transferred onto polyvinylidene fluoride membranes (Millipore). After blocking, the membranes were incubated with primary antibodies (Table S1) and then with anti-rabbit IgG and anti-mouse IgG. The proteins were visualized using the BeyoECL Plus chemiluminescence detection kit (Beyotime Institute of Biotechnology, Beyotime, Shanghai, China). The enhanced chemiluminescence signals were scanned using a FluorChem M apparatus (Protein Simple, Inc., Santa Clara, California), and the band densities were analyzed with ImageJ software.

2.17 | Automated capillary Western blotting

All operations were performed strictly following the user guide. In brief, the enteroids were lysed in RIPA lysis buffer, and the protein lysates were diluted and mixed with 5× fluorescent markers and boiled for 5 minutes, as was a biotinylated ladder, then stored on ice. The lysates and other reagents were poured into assay plates. The plate was loaded into the instrument, and the Western blotting assay protocol was configured to run automatically. The data were analyzed by Compass software 3.1 (Protein Simple, San Jose, California).

2.18 | Molecular docking

The three-dimensional crystal structures of STa (ID: 1ETN) and FZD7 cysteine-rich region (ID: 5 T44) were downloaded from the Protein Data Bank (https://www.rcsb.org/) and loaded to Sybyl x2.1. Meanwhile, PyMOL was used to draw the three-dimensional structure of STa and FZD7, which was further preoptimized using the free version of GROMACS 5.1.4 from ChemAxon with an MM force field. MolDock score functions were used with a 0.3 Å grid resolution. Before the calculations of the subject compounds, the Sybyl x2.1 software was benchmarked for docking the STa to FZD7.

2.19 | Statistical analysis

The data are presented as the mean ± SEM. The data were analyzed using SPSS software version 19.0 (SPSS, Inc., Chicago, Illinois). The t test and Duncan's multiple range test were used to evaluate the differences between two groups or multiple groups after performing normality testing, respectively. P values <.05 were considered significant: $*P < .05$.

3 | RESULTS

3.1 | Acute exposure to STp disrupts intestinal epithelial integrity and induces spheroid formation in vivo

To assess the effect of STp on intestinal integrity, mice were orally administrated 5.0 mg/kg BW STp or PBS. The results showed that STp treatment led to prominent edema in the small intestine (Figures 1A and S1A) and a decrease in jejunum mass but had no significant effect on the mass of the duodenum or ileum (Figure 1B). Besides, STp-induced jejunal integrity disruption was reflected in the decrease in TEER values and DAO activity (Figure 1C,D). As observed through scanning electron microscopy, the jejuna of the STp-treated mice displayed severe multifocal apical necrosis in the villi (Figure 1E). The expression of tight junction (TJ) proteins ZO-1, Occludin, and

FIGURE 1　Acute exposure to STp disrupts intestinal epithelial integrity and induces spheroid formation in vivo. A, STp-induced small intestinal edema. A total of five pairs of male mice with similar body weights were administered either 0 (control, CON) or 5.0 mg/kg body weight (BW) STp (dissolved in PBS) through gavage, and after 6 hours, severe intestinal edema was induced by STp. B, The intestinal mass of the mice treated with PBS or STp; n = 5 mice per group. C, Transepithelial cell resistance (TEER) of the jejuna of mice treated with PBS or STp; n = 5 mice per group. D, Diamine oxidase (DAO) activity of the jejuna of mice treated with PBS or STp; n = 5 mice per group. E, Scanning electron microscope of the jejuna of mice treated with PBS or STp. Scale bars = 100 μm (upper: ×250) and 20 μm (lower: ×1000); n = 3 mice per group. F, G, Western blotting analysis results are showing ZO-1, occludin, and claudin-1 expression in the jejuna of mice; n = 3 mice per group. H-J, The jejuna were stained with Villin (green), MUC2 (Red), and LYZ (red), and the nuclei were stained with 4',6-diamidino-2-phenylindole (DAPI, blue). MUC2- and LYZ-positive cells were mostly distributed in the villous region and the crypt region, respectively; n = 5 mice per group. Scale bar = 100 μm. K, Images of ex vivo culture of crypts isolated from the jejuna of mice in the CON and STp groups. Scale bars = 500 μm. L, Enteroid-forming efficiency at 120 hours, n = 12 wells from three mice per group. M, Enteroid-budding efficiency at 120 hours, n = 12 wells from three mice per group. N,O, Western blotting results are showing Active β-catenin, β-catenin, Lgr5, and PCNA expression in the mouse enteroids; n = 3 mice per group. Data are the mean ± SEM; comparisons are performed with t tests. $*P < .05$. DAO, diamine oxidase; PBS, phosphate-buffered saline; TEER, trans-epithelial electrical resistance
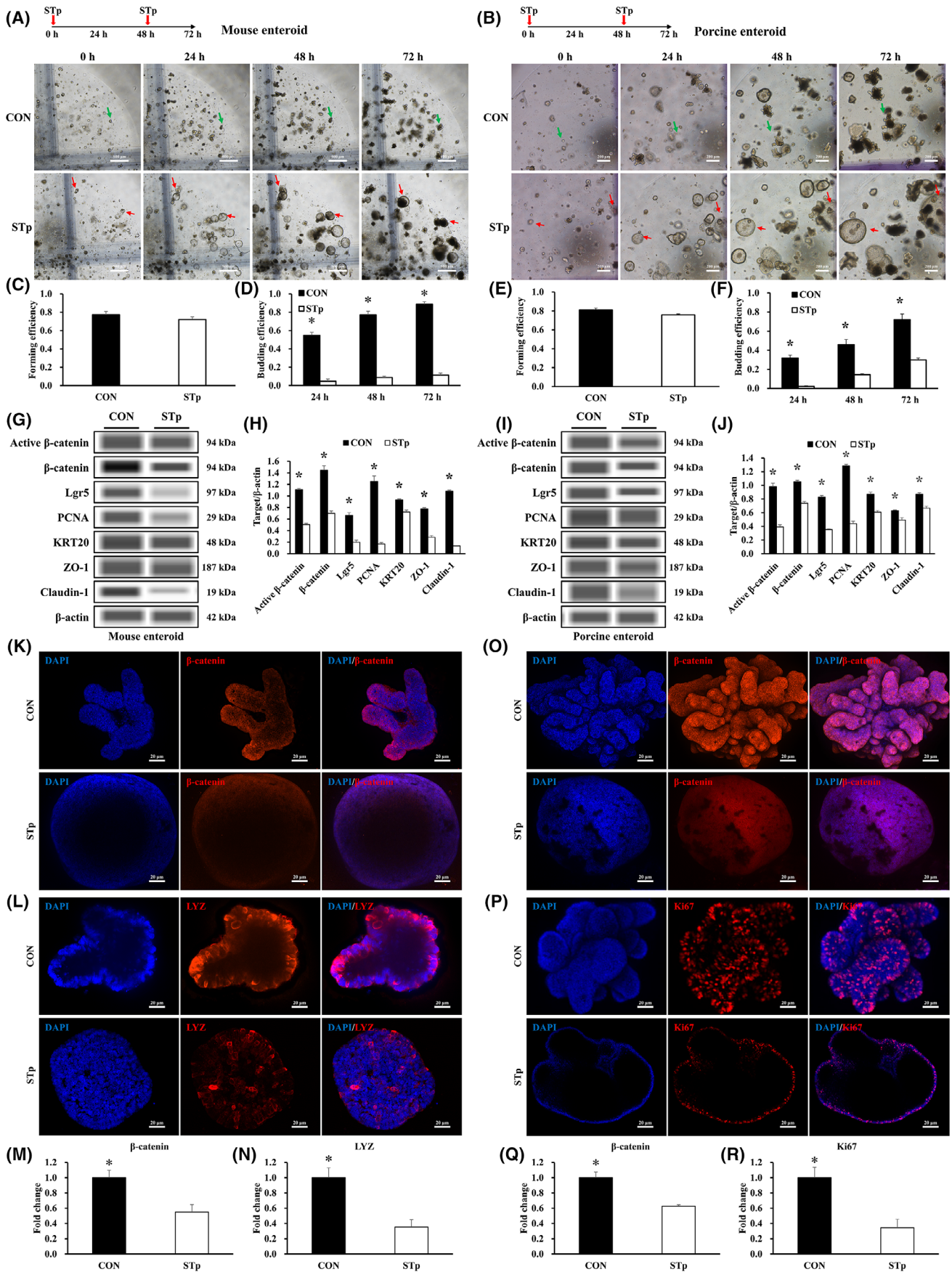
FIGURE 2   Legend on next page.

claudin-1, which represent the physical barrier of the intestinal epithelium, were significantly decreased in the jejuna (Figure 1F,G) and crypts (Figure S1B,C). Correspondingly, compared with that of the control group, the number of MUC2+ (goblet cell) and LYZ+ (Paneth cell) cells, which are essential components in the intestinal epithelial chemical barrier and immune barrier, respectively, in the STp group was significantly reduced (Figure 1H-J), as was the fluorescence signal intensity of Villin (Figure 1H). In addition, the crypts isolated from the jejuna of the mice treated with or without STp were cultured in the same conditional medium. We found that, after acute exposure to STp, crypt stem cells were induced to generate predominantly large hollow spheroids (also referred to as enterospheres or spheres) (Figure 1K). Evidence from the quantification of enteroids and spheroids showed that, after 120 hours in culture, STp decreased enteroid-budding efficiency but had no effect on enteroid forming-efficiency (Figure 1L,M). The levels of Active β-catenin, β-catenin, Lgr5, and PCNA expression in the spheroids were significantly downregulated after STp exposure (Figures 1N,O and S1D).

3.2 | STp reduces the activity of ISCs ex vivo

To further verify the effect of STp on the stimulation of spheroids, seeded mouse and porcine enteroids were incubated with STp. As expected, compared to that of the control group, the volume of spheroids increased rapidly with the prolongation of treatment time in the STp group (Figures 2A,B and S2A). And likewise, the enteroid-forming efficiency in the STp group did not change significantly (Figure 2C,E), but enteroid-budding efficiency was significantly diminished (Figures 2D,F and S2B). Moreover, the levels of Active β-catenin, β-catenin, Lgr5, PCNA, KRT20, ZO-1, and claudin-1 expression in the enteroids were significantly downregulated under STp exposure (Figure 2G-J), as was the fluorescence signal intensity of β-catenin (Figure 2K,M) and LYZ (Figure 2L,N) in mouse enteroids, as well as β-catenin (Figure 2O,Q) and Ki67 (Figure 2P,R) in porcine enteroids.

3.3 | STp inhibits intestinal epithelial cell proliferation and induces its apoptosis in vitro

Then, the effect of STp on intestinal epithelial cell proliferation and apoptosis was examined in the MODE-K, IPEC-J2, and CMT-93 cell models. The results showed that the OD values were decreased after

exposure to 400 ng/mL STp for 48 and 72 hours (Figures 3A,B and S3A), and the change in cell numbers showed the same tendency as the OD values (Figures 3C,D and S3B). Meanwhile, the EdU incorporation assays and immunofluorescence staining of Ki67 showed that STp exposure for 48 hours led to a significant decrease in the number of EdU+ and Ki67+ cells in the MODE-K (Figure 3E,F), IPEC-J2 (Figure 3G,H), and CMT-93 cells (Figure S3C-E). The results from the Western blotting analysis showed that exposure of the CMT-93 cells to STp for 48 hours resulted in a significant decrease in the PCNA protein level (Figure S3F,G).

Furthermore, the rates of late apoptotic cells (Q2) and total apoptotic cells (Q2 + Q4), as detected by fluorescence activated cell sorting (FACS), increased significantly in the STp group (Figure S4A-D). However, there was no significant effect on the early apoptotic rate (as shown in Q4) between the control group and the STp group (Figure S4A-D). Likewise, STp upregulated Cleaved caspase3 expression in the MODE-K (Figure S4E,F) and IPEC-J2 cells (Figure S4G,H). The levels of fluorescence signal intensity of Cleaved caspase3 in MODE-K (Figure S4I,J) and IPEC-J2 cells (Figure S4K,L) were consistent with that of Western blotting analysis.

3.4 | STp damages the intestinal epithelial cell barrier

To investigate the intestinal barrier dysfunction induced by STp, a confluent monolayer of MODE-K, IPEC-J2, and CMT-93 cells were exposed to STp for 24, 48, 72, and 96 hours. As shown in Figures 4A, B and S5A, STp induced a significant decrease in the TEER value. The levels of the TJ proteins, including ZO-1 and claudin-1, were analyzed by Western blotting (Figures 4C-F and S5D,E) and fluorescence signal (Figures 4G-J and S5B,C). The results showed that these proteins were downregulated in the MODE-K, IPEC-J2, and CMT-93 cells that had been exposed to STp compared to the proteins in the control group.

3.5 | Wnt/β-catenin is involved in STp-induced intestinal epithelial cell damage

Similarly, the Wnt/β-catenin pathway was significantly downregulated in the MODE-K and IPEC-J2 cells after exposure to 400 ng/mL STp for 48 hours. Specifically, the p-β-catenin level was increased, and the

FIGURE 2 STp treatment inhibits the activity of intestinal stem cells. A,B, Images of mouse enteroids (A) and porcine enteroids (B) that were treated with/without STp (400 ng/mL) for 72 hours (enteroid: green arrow; spheroid: red arrow). Scale bars = 500 μm (A) and 200 μm (B). C,D, Mouse enteroid-forming efficiency (C) at 72 hours and enteroid-budding efficiency (D) at 24, 48, and 72 hours. E,F, Porcine enteroid-forming efficiency (E) at 72 hours and enteroid-budding efficiency (F) at 24, 48, and 72 hours. G-J, Western blotting results are showing Active β-catenin, β-catenin, Lgr5, PCNA, ZO-1, and claudin-1 expression in mouse enteroids (G, H) and porcine enteroids (I, J). K,M, Mouse enteroids were stained with β-catenin (red). Nuclei were stained with 4',6-diamidino-2-phenylindole (DAPI, blue). Scale bar = 20 μm. L,N, Mouse enteroids were stained with lysozyme (LYZ, red). Nuclei were stained with DAPI (blue). Scale bar = 20 μm. O,Q, Porcine enteroids were stained with β-catenin (red). Nuclei were stained with DAPI (blue). Scale bar = 20 μm. P,R, Porcine enteroids were stained with Ki67 (red). Nuclei were stained with DAPI (blue). Scale bar = 20 μm. Data are the mean ± SEM; comparisons are performed with t tests. *P < .05. At least three independent experiments were performed
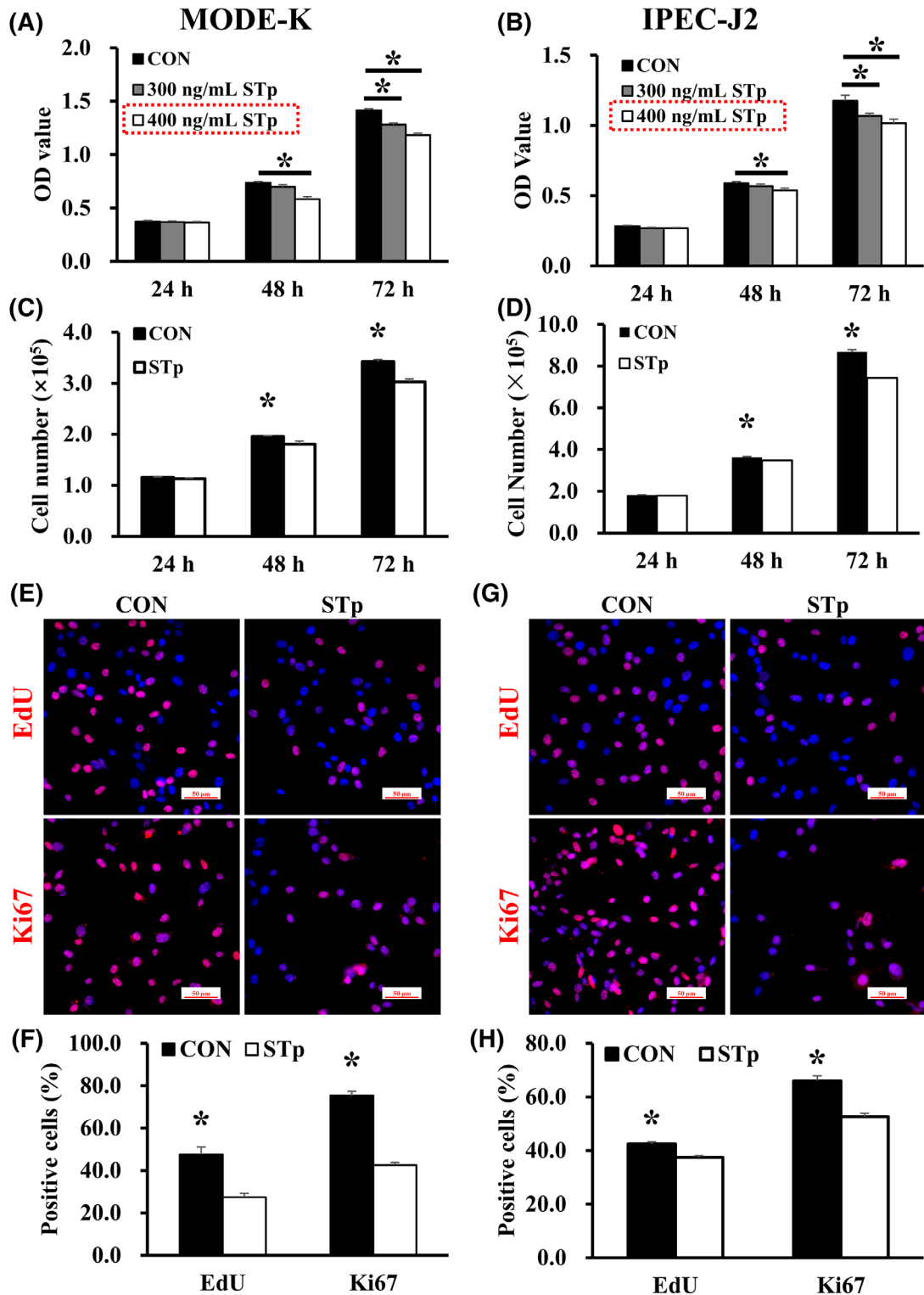
FIGURE 3 STp treatment inhibits the viability and proliferation of the intestinal epithelial cells. A,B, MODE-K (A) and IPEC-J2 (B) cells were treated with 0, 300, and 400 ng/mL STp. The cell viability in the three groups at 24, 48, and 72 hours was measured by the MTT assay, n = 20 wells per group. C,D, MODE-K (C) and IPEC-J2 (D) cells were treated with 400 ng/mL STp. The cell proliferation in the two groups at 24, 48, and 72 hours was assessed by the cell count assay, n = 6 wells per group. E-H, MODE-K (E, F) and IPEC-J2 (G, H) cells were stained with EdU (red) or Ki67 (red) at 48 hours. Nuclei were stained with 4',6-diamidino-2-phenylindole (DAPI, blue). Scale bar = 50 μm. Data are the mean ± SEM; comparisons are performed with t tests (two groups) or analysis of variance (three groups). *P < .05. At least three independent experiments were performed
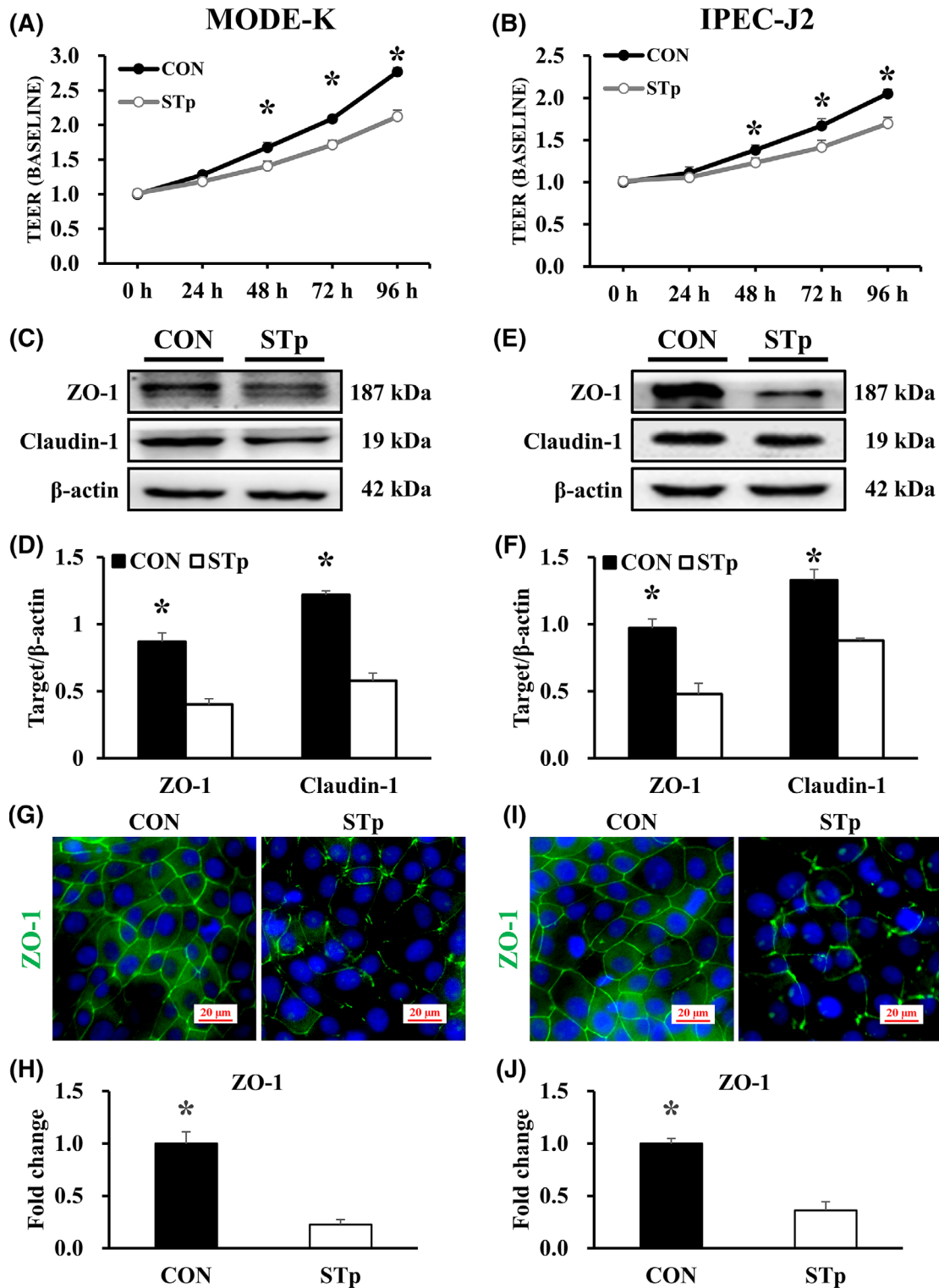
FIGURE 4   STp treatment damages the intestinal epithelial cell barrier. A,B, MODE-K (A) and IPEC-J2 (B) cells were treated with 400 ng/mL STp. The trans-epithelial electrical resistance (TEER) of cell monolayers was tested using Transwell filters. C-F, Western blotting results of ZO-1 and claudin-1 at 48 hours in MODE-K (C, D) and IPEC-J2 (E, F) cells. G-J, MODE-K (G, H) and IPEC-J2 (I, J) cells were stained with ZO-1 (green). Nuclei were stained with 4',6-diamidino-2-phenylindole (DAPI, blue). Scale bar = 20 μm. Data are the mean ± SEM; comparisons are performed with tests. *$P < .05$. At least three independent experiments were performed

levels of Active β-catenin, β-catenin, TCF4, cyclin D1, and c-Myc were decreased (Figure 5A-D). Furthermore, the fluorescence signal intensity of Active β-catenin was reduced by STp (Figure 5E-H).

To validate the role of the Wnt/β-catenin pathway in the repair of the intestine after injury, IPEC-J2 cells were treated with STp at 0 hour and RSPO1 at 24 hours (Figure 6A). RSPO1 administered at
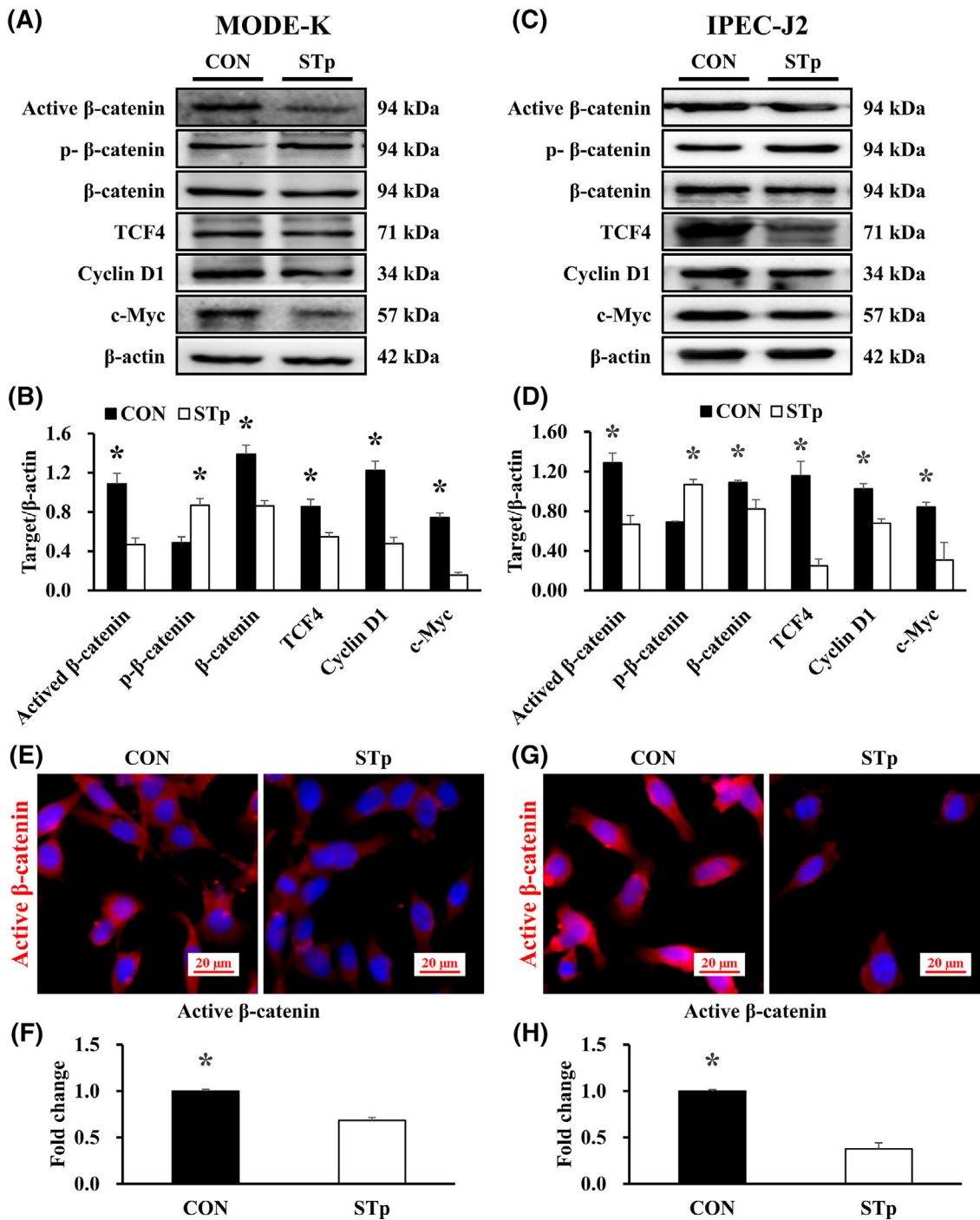
FIGURE 5 STp treatment inhibits the Wnt/β-catenin signaling pathway. A-D, Western blotting results are showing the Wnt/β-catenin pathway-related protein expression at 48 hours in the MODE-K (A, B) and IPEC-J2 (C, D) cells. E-H, MODE-K (E, F) and IPEC-J2 (G, H) cells were stained with Active β-catenin (red). Nuclei were stained with 4',6-diamidino-2-phenylindole (DAPI, blue). Scale bar = 20 μm. Data are the mean ± SEM; comparisons are performed with *t* tests (two groups). *$P < .05$. At least three independent experiments were performed

25 ng/mL significantly increased cell viability (Figure 6B), BrdU⁺ cell number (Figure 6C), and had upregulated the expression of Active β-catenin (Figure 6D,E) and β-catenin (Figure 6F,G) within 96 hours. The results of immunofluorescence showed that RSPO1 inhibited the fluorescence signal intensity of ZNRF3, which can promote the degradation of the Wnt membrane receptor FZDs, while STp had no

significant effect on it (Figure S6A,B). Besides, the recombinant plasmid pCDH-CMV-β-catenin-MCS-EF1-GFP-puro was identified with restriction endonuclease analysis (Figure S7A-C), and Western blotting confirmed that β-catenin was overexpressed (OE) in the IPEC-J2 cells (Figure 6H,I). After treated with 400 ng/mL STp for 48 hours, the expression level of Active β-catenin, β-catenin, TCF4, Cyclin D1,
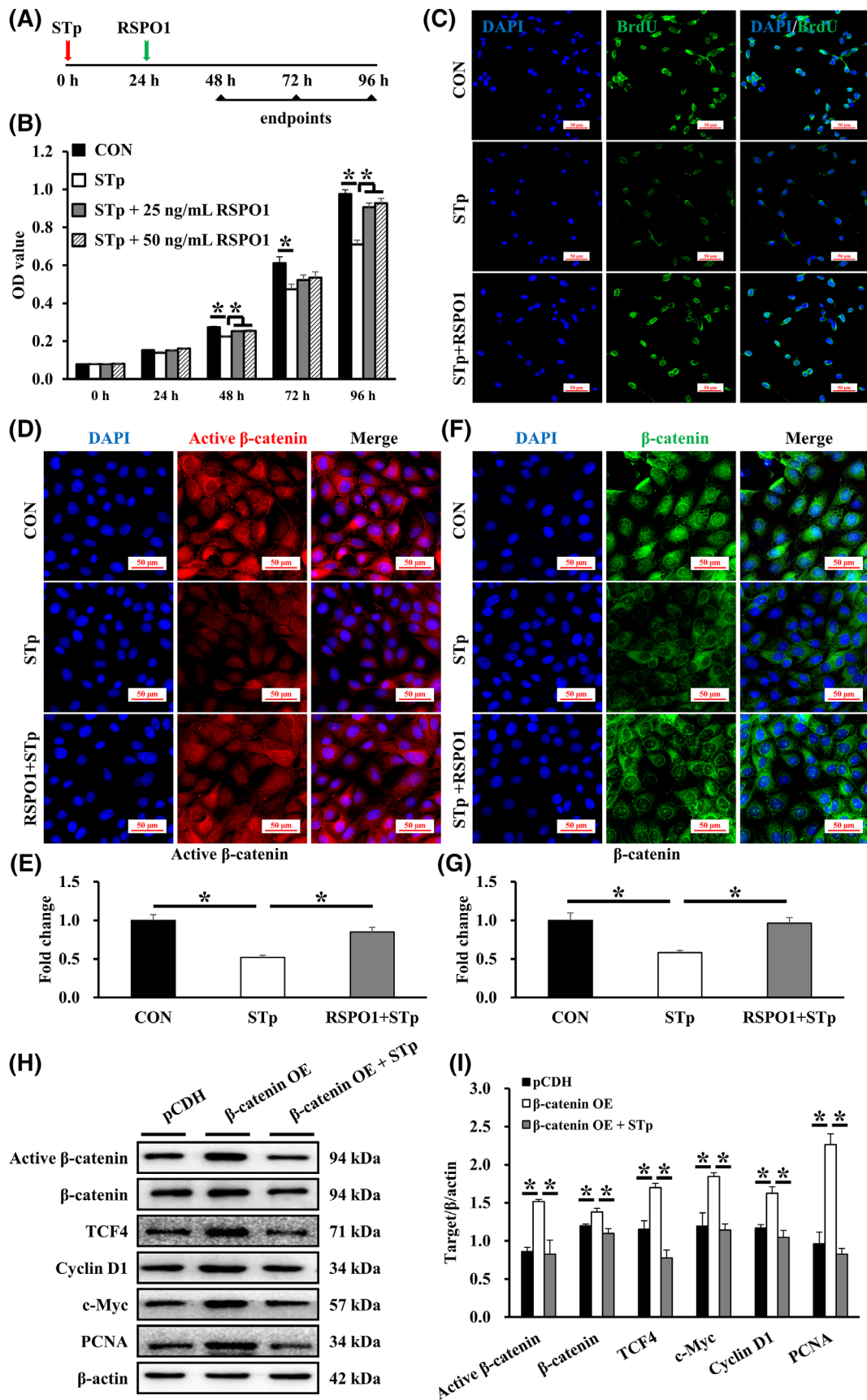
FIGURE 6 Legend on next page.

FIGURE 7 STp inhibits Wnt/β-catenin activity by downregulating membrane receptor FZD7. A,B, Binding mode of parabens to STa-FZD7. The protein is shown in cartoon form. Parabens and surrounding residues are represented in stick form. The dashed lines indicate the formation of hydrogen bonds. C,J, Western blotting results are showing FZD7 expression in mouse enteroids (C, D), porcine enteroids (E, F), MODE-K cells (G, H), and IPEC-J2 cells (I, J) at 48 hours after STp treatment. K-N, MODE-K (K, L) and IPEC-J2 (M, N) cells were stained with FZD7 (red). Nuclei were stained with 4',6-diamidino-2-phenylindole (DAPI, blue). Scale bar = 20 μm. O,P, Western blotting results are showing the expression of Wnt/β-catenin pathway-related protein and Ki67 at 48 hours in the IPEC-J2 cells transfected with pCDH-CMV-β-catenin-MCS-EF1-GFP-puro. Q-R, IPEC-J2 cells were stained with EdU (red) at 48 hours. Nuclei were stained with DAPI (blue). Scale bar = 20 μm. S, Our model depicts the damage induced by STp on the intestinal mucosal epithelial integrity via the inhibition of ISCs. Data are the mean ± SEM; comparisons are performed with *t* tests or analysis of ANOVA (three groups). *$P < .05$. At least three independent experiments were performed. ANOVA, analysis of variance; ISCs, intestinal stem cells
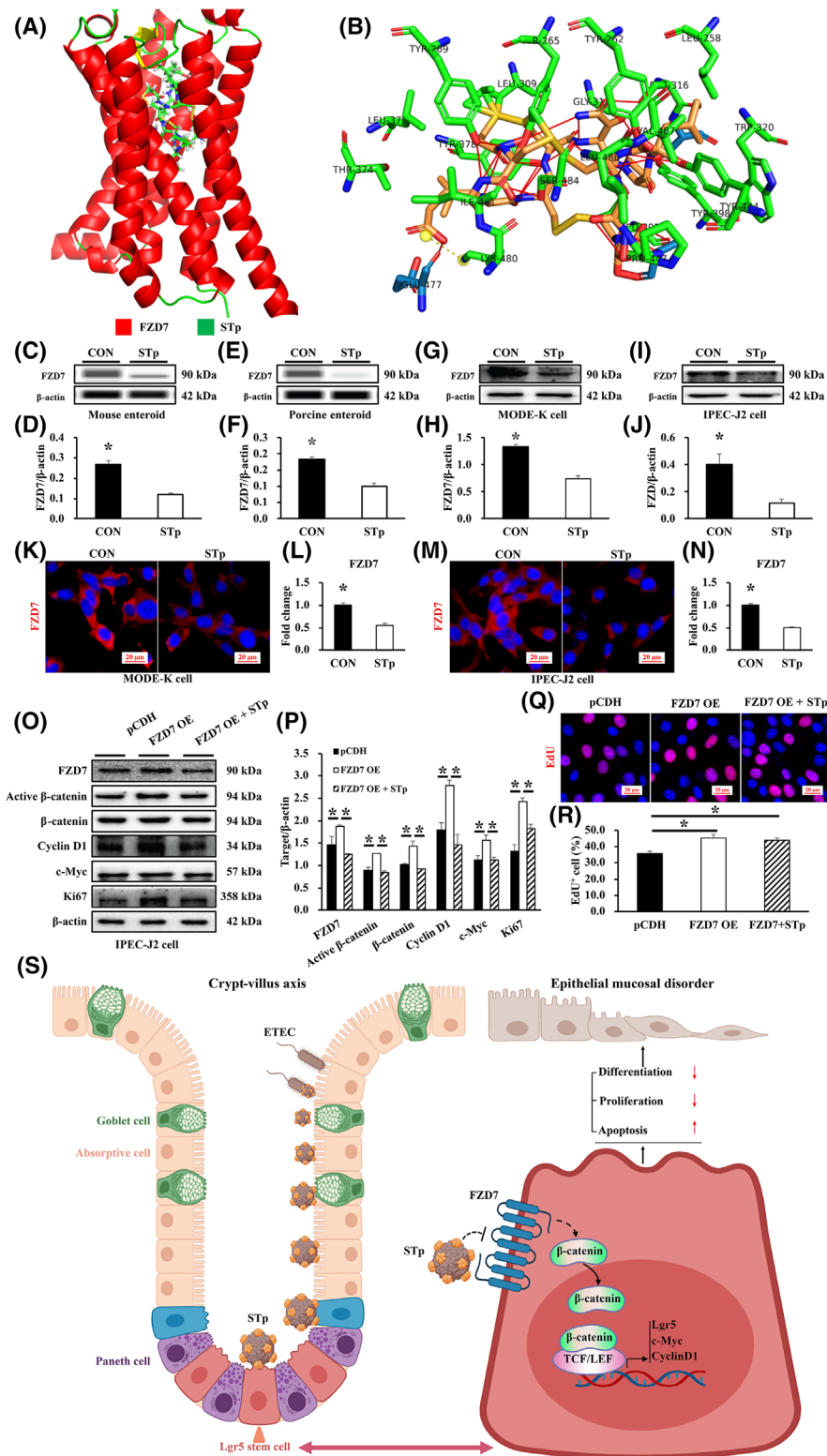
FIGURE 6 Wnt/β-catenin signaling activation prevents STp-induced IPEC-J2 cell damage. A, Experimental procedure: IPEC-J2 cells were treated with 400 ng/mL STp at 0 hour and then supplemented with R-spondin 1 (RSPO1) at 24 hours, and the cell samples were collected at 96 hours. B, IPEC-J2 cells were treated with STp (400 ng/mL) and RSPO1 (25 or 50 ng/mL). The cell viability in the four groups at 0, 24, 48, 72, and 96 hours were measured by MTT assays, n = 20 wells per group. C, IPEC-J2 cells were stained with BrdU (green) at 96 hours. Nuclei were stained with 4',6-diamidino-2-phenylindole (DAPI, blue). Scale bar = 50 μm. D-G, IPEC-J2 cells were stained with Active β-catenin (red) (D, E) and β-catenin (green) (F, G). Nuclei were stained with DAPI (blue). Scale bar = 50 μm. F,G, Western blotting results are showing the expression of Wnt/β-catenin pathway-related protein and PCNA at 48 hours in IPEC-J2 cells with β-catenin overexpression (OE), which were transfected with pCDH-CMV-β-catenin-MCS-EF1-GFP-puro. Data are the mean ± SEM; comparisons are performed with *t* tests (two groups) or ANOVA (multiple groups). *$P < .05$. At least three independent experiments were performed. ANOVA, analysis of variance

c-Myc, and PCNA in β-catenin-OE cells returned to the level in the empty plasmid group (Figure 6H,I).

3.6 | STp inhibits Wnt/β-catenin activity by downregulating membrane receptor FZD7

We confirmed that STp inhibited the Wnt/β-catenin signaling pathway, but it is not clear whether STp directly or indirectly affects it. The molecular simulation is a useful tool that, when used in conjunction with experimental results, can develop our understanding of the STp-FZD7 interaction. The docking results from the MVD program predicted that there were 22 hydrophobic interactions, 34 hydrogen bonds, 1 water bridge, and 1 salt bridge between STa and the cysteine-rich region of FZD7, suggesting that STp might bind to the subdomain of FZD7. The docking calculations showed the lowest binding energy conformer, which is shown in Figure 7A,B. Western blotting showed that STp significantly inhibited FZD7 expression in mouse enteroids (Figure 7C,D) and porcine enteroids (Figure 7E,F), as well as in MODE-K (Figure 7G,H) and IPEC-J2 cells (Figure 7I,J). The results of FZD7 fluorescence signal intensity in MODE-K (Figure 7K,L) and IPEC-J2 cells (Figure 7M,N) were consistent with that of Western blotting. Furthermore, the FZD7 recombinant plasmid was constructed (Figure S7D-F), and FZD7 OE was confirmed in IPEC-J2 cells (Figure 7O,P). STp treatment for 48 hours inhibited Wnt/β-catenin signaling pathway and Ki67 expression in IPEC-J2 cells with FZD7 OE (Figure 7O,P). And the EdU$^+$ cell rates in the group of FZD7 OE and FZD7 OE + STp were significantly higher than those in the pCDH group (Figure 7Q,R). These results suggest that STp might inhibit the Wnts-initiated classic signal transduction pathway, at least partially, by downregulating FZD7.

4 | DISCUSSION

ETEC is one of the most common pathogens to cause enteric diseases during the weaning period and in infancy.[17,18] On the one hand, ETEC infection induces pro-inflammatory and responses in intestinal epithelial cells.[19,20] On the other hand, ETEC-produced STs can bind to the extracellular domain of guanylyl cyclase (cGMPase), which is located on the enterocyte surface, to result in the accumulation of cGMP due to the similar three-dimensional structure with guanylin and uroguanylin.[21] Subsequently, the cGMP regulates channels' regulator by cGMP-dependent Protein Kinase II (PKGII), inhibits sodium chloride absorption and accelerates chloride secretion.[5] Loos et al showed that the fluid secreted by the mid-jejunal segments of piglets increased after perfusing with 50 nmol/L STa for 6 hours.[18] Results of STp induced intestinal edema we observed support those early studies. Unsurprisingly, acute exposure to STp damaged intestinal structure and mechanical barrier. It is well known that the intestinal mucosal epithelial layer represents the first line of defense against luminal contents, with intercellular TJs critical for maintaining paracellular barrier function and mediating paracellular ion and water

transport between adjacent cells and specialized secretory cell types, such as goblet cells and Paneth cells, necessary for secreting the antimicrobial factors that prevent tissue damage.[22,23]

ISCs can spontaneously differentiate into all epithelial cell types, and collectively, they maintain intestinal epithelial homeostasis.[24] Our results showed that the decrease in the expression of absorptive cells, goblet cells, and Paneth cells markers suggested that the differentiation ability of ISCs might be suppressed by exposure to STp. However, these phenomena have rarely been mentioned in other studies before. In an unexpected finding, STp triggered ISCs to give rise to the unique three-dimensional spherical structure, which showed a different appearance from enteroids with proliferative crypt-like bud domains. It is noteworthy that STa induces net accumulation of fluid by inducing secretion and blocking absorption, thus producing volume expansion in the enteroid lumen.[5] Interestingly, under identical culture conditions, Bmi1$^+$ cells predominantly generated large hollow spheroids, but the Lgr5$^+$ cells predominately generated enteroids.[6] Furthermore, compared with the enteroids, the spheroids showed reduced mRNA abundance of the active-cycling ISC marker Lgr5 and Paneth cell marker LYZ.[6,25] Coincidentally, our study revealed that the expression level of Lgr5 and LYZ in the enteroids was significantly greater than it was in the STp-induced spheroids. These findings suggest that STp reduces the activity of Lgr5 stem cells and might induce their transformation to Bmi1 stem cells. A recent study showed that arachidonic acid negatively regulated intestinal epithelial cell differentiation and induced mouse enteroids to develop into cystic structures.[26] Although enteroids are Wnt-dependent and spheroids can grow in the RSPO1-depleted medium, these spheroids retained the potential to form buds in the presence of RSPO1.[7] We also found that STp suppressed the Wnt/β-catenin signaling pathway. Thus, it is likely that re-expression of the Wnt-target gene Lgr5 and transition into a Wnt-dependent state is necessary for bud formation.[27] We reasoned that analyses using ex vivo three-dimensional culture would provide a simple system that would permit the temporal tracking of the transition of spheroids to enteroids. This process may be analogous to the regeneration and repair of the intestinal epithelium in response to injury and diarrhea.

Wnt/β-catenin-dependent ISCs are critical for maintaining intestinal epithelial integrity.[28-30] Previous studies have demonstrated that blocking Wnt/β-catenin signaling inhibited cell proliferation and induced cell apoptosis.[31,32] However, how STp acts on the Wnt/β-catenin signaling pathway to influence the proliferation and apoptosis of intestinal epithelial cells is unknown. Coincidentally, Flanagan et al showed that FZD7 was enriched in Lgr5$^+$ stem cells, and its loss in adult intestinal epithelium decreased basal Wnt signaling and led to ISC loss in vivo and organoid death in vitro, indicating that FZD7 is required for robust Wnt-dependent processes in ISCs.[33] Interestingly, molecular docking analysis predicted the possible sites where STp might bind to the Wnt receptor FZD7. Although we confirmed that FZD7 expression was suppressed by STp, direct experimental evidence that they interact through the predicted active center to be verified in further study. Undeniably, as the level of FZD7 decreases, cytosolic β-catenin is subsequently marked for degradation by a protein complex that includes CK1α, GSK3, Axin1, and APC. The TCF proteins are associated with transcriptional

repressors of the Groucho/transducin-like enhancer of split family that blocks the expression of Wnt-responsive genes, such as cyclin D1, c-Myc, and Lgr5.[34] Ultimately, STp inhibited cell proliferation and induced cell apoptosis in the MODE-K and IPEC-J2 cell models. A model of RSPO1-induced Wnt/β-catenin signaling activation illustrates that RSPO1 inhibits degradation of the FZD receptors by antagonizing ZNRF3,[35] which is consistent with the result that RSPO1 suppresses ZNRF3 fluorescence signal intensity in our studies. Notably, activation of Wnt/β-catenin signaling via RSPO1 supplementation increased STp-treated intestinal epithelial cell viability, which suggests that RSPO1 might be useful in the repair of STp-induced intestinal injury or diarrhea.

5 | CONCLUSION

In summary, our findings demonstrate that STp inhibits ISC expansion to disrupt the integrity of intestinal mucosa through the down-regulation of the Wnt/β-catenin signaling pathway (Figure 7S). The dysfunction of ISC is associated with the occurrence and development of diarrhea. It supports the notion that restoring Wnt-dependent ISCs is a promising therapeutic target for the intervention of ETEC.

CONFLICT OF INTEREST

The authors declared no potential conflicts of interest.

AUTHOR CONTRIBUTIONS

J.-Y.Z.: conception and design, data analysis and interpretation, manuscript writing; D.-G.H.: collection and assembly of data; C.-Q.G., H.-C.Y., S.-G.Z.: manuscript editing; X.-Q.W.: conception and design, final approval of the manuscript; All authors read and approved the final manuscript.

DATA AVAILABILITY STATEMENT

The data that support the findings of this study are available from the corresponding author upon reasonable request.

ORCID

Xiu-qi Wang https://orcid.org/0000-0003-2033-9485

REFERENCES

1. Troeger C, Forouzanfar M, Rao PC, et al. Estimates of global, regional, and national morbidity, mortality, and aetiologies of diarrhoeal diseases: a systematic analysis for the Global Burden of Disease Study 2015. *Lancet Infect Dis*. 2017;17:909-948.
2. Isidean SD, Riddle MS, Savarino SJ, Porter CK. A systematic review of ETEC epidemiology focusing on colonization factor and toxin expression. *Vaccine*. 2011;29:6167-6178.
3. Wenneras C, Erling V. Prevalence of enterotoxigenic *Escherichia coli*-associated diarrhoea and carrier state in the developing world. *J Health Popul Nutr*. 2004;22(4):370-382.
4. Nagy B, Fekete PZ. Enterotoxigenic *Escherichia coli* in veterinary medicine. *Int J Med Microbiol*. 2005;295:443-454.
5. Pattison AM, Blomain ES, Merlino DJ, et al. Intestinal enteroids model guanylate cyclase C-dependent secretion induced by heat-stable enterotoxins. *Infect Immun*. 2016;84:3083-3091.
6. Smith NR, Swain JR, Davies PS, et al. Monoclonal antibodies reveal dynamic plasticity between Lgr5- and Bmi1-expressing intestinal cell populations. *Cell Mol Gastroenterol Hepatol*. 2018;6:79-96.
7. Zhou JY, Huang DG, Zhu M, et al. Wnt/β-catenin-mediated heat exposure inhibits intestinal epithelial cell proliferation and stem cell expansion through endoplasmic reticulum stress. *J Cell Physiol*. 2020;235:5613-5627.
8. Li XG, Wang Z, Chen RQ, et al. Lgr5 and Bmi1 increase pig intestinal epithelial cell proliferation by stimulating Wnt/β-catenin signaling. *Int J Mol Sci*. 2018;19:1036-1047.
9. Li XG, Zhu M, Chen MX, et al. Acute exposure to deoxynivalenol inhibits porcine enteroid activity via suppression of the Wnt/β-catenin pathway. *Toxicol Lett*. 2019;305:19-31.
10. Zhou JY, Wang Z, Zhang SW, et al. Methionine and its hydroxyl analogs improve stem cell activity to eliminate deoxynivalenol-induced intestinal injury by reactivating Wnt/β-catenin signaling. *J Agr Food Chem*. 2019;67:11464-11473.
11. Zhou JY, Zhang SW, Lin HL, Gao CQ, Yan HC, Wang XQ. Hydrolyzed wheat gluten improves intestinal stem cell proliferation and differentiation exposed to deoxynivalenol by regulating the Wnt/β-catenin signaling in mice. *Food Chem Toxicol*. 2019;131:110579-110589.
12. Son JW, Kim YJ, Cho HM, et al. Promoter hypermethylation of the CFTR gene and clinical/pathological features associated with non-small cell lung cancer. *Respirology*. 2011;16:1203-1209.
13. Strubberg AM, Liu J, Walker NM, et al. Cftr modulates Wnt/β-catenin signaling and stem cell proliferation in murine intestine. *Cell Mol Gastroenterol Hepatol*. 2017;5(3):253-271.
14. Zhou JY, Huang DG, Qin YC, et al. mTORC1 signaling activation increases intestinal stem cell activity and promotes epithelial cell proliferation. *J Cell Physiol*. 2019;234:19028-19038.
15. Li CM, Yan HC, Fu HL, Xu GF, Wang XQ. Molecular cloning, sequence analysis, and function of the intestinal epithelial stem cell marker Bmi1 in pig intestinal epithelial cells. *J Anim Sci*. 2014;92:85-94.
16. Zhu M, Qin YC, Gao CQ, Yan HC, Li XG, Wang XQ. Extracellular glutamate-induced mTORC1 activation via the IR/IRS/PI3K/Akt pathway enhances the expansion of porcine intestinal stem cells. *J Agric Food Chem*. 2019;67:9510-9521.
17. Donowitz M, Alpers DH, Binder HJ, et al. Translational approaches for pharmacotherapy development for acute diarrhea. *Gastroenterology*. 2012;142:1-9.
18. Loos M, Hellemans A, Cox E. Optimization of a small intestinal segment perfusion model for heat-stable enterotoxin A induced secretion in pigs. *Vet Immunol Immunopathol*. 2013;52:82-86.
19. Ren WK, Yin J, Duan JL, et al. Mouse jejunum innate immune responses altered by enterotoxigenic *Escherichia coli* (ETEC) infection. *Microbes Infect*. 2014;16:954-961.
20. Bin P, Tang ZY, Liu SJ, et al. Intestinal microbiota mediates Enterotoxigenic *Escherichia coli*-induced diarrhea in piglets. *BMC Vet Res*. 2018;14:385-397.
21. Xia YY, Bin P, Liu SJ, et al. Enterotoxigenic *Escherichia coli* infection promotes apoptosis in piglets. *Microb Pathog*. 2018;125:290-294.
22. Chelakkot C, Ghim J, Ryu SH. Mechanisms regulating intestinal barrier integrity and its pathological implications. *Exp Mol Med*. 2018;50:1-9.
23. Huang GP, Li XQ, Lu D, et al. Lysozyme improves gut performance and protects against enterotoxigenic *Escherichia coli* infection in neonatal piglets. *Vet Res*. 2018;49:20-30.
24. Gehart H, Clevers H. Tales from the crypt: new insights into intestinal stem cells. *Nat Rev Gastroenterol Hepatol*. 2019;16:19-34.

25. Khalil HA, Nan YL, Brinkley G, et al. A novel culture system for adult porcine intestinal crypts. *Cell Tissue Res*. 2016;365:123-134.

26. Wang QY, Lin YY, Sheng XL, et al. Arachidonic acid promotes intestinal regeneration by activating Wnt signaling. *Stem Cell Reports*. 2020;15:374-388.

27. Yin XL, Farin HF, Es JHV, et al. Niche-independent high-purity cultures of Lgr5+ intestinal stem cells and their progeny. *Nat Methods*. 2014;11:106-112.

28. Andersson-Rolf A, Zilbauer M, Koo BK, Clevers H. Stem cells in repair of gastrointestinal epithelia. *Physiology*. 2017;32:278-289.

29. Merenda A, Fenderico N, Maurice MM. Wnt signaling in 3D: recent advances in the applications of intestinal organoids. *Trends Cell Biol*. 2020;30:60-73.

30. Zhou JY, Lin HL, Wang Z, et al. Zinc L-aspartate enhances intestinal stem cell activity to protect the integrity of the intestinal mucosa against deoxynivalenol through activation of the Wnt/β-catenin signaling pathway. *Environ Pollut*. 2020;262:114290.

31. Hu YD, Yu KK, Wang G, et al. Lanatoside C inhibits cell proliferation and induces apoptosis through attenuating Wnt/β-catenin/c-Myc signaling pathway in human gastric cancer cell. *Biochem Pharmacol*. 2018;150:280-292.

32. Li B, Lee C, Cadete M, et al. Impaired Wnt/β-catenin pathway leads to dysfunction of intestinal regeneration during necrotizing enterocolitis. *Cell Death Dis*. 2019;10:1-11.

33. Flanagan DJ, Phesse TJ, Barker N, et al. Frizzled7 functions as a Wnt receptor in intestinal epithelial Lgr5+ stem cells. *Stem Cell Reports*. 2015;4:759-767.

34. Yan KS, Janda CY, Chang J, et al. Non-equivalence of Wnt and R-spondin ligands during Lgr5+ intestinal stem-cell self-renewal. *Nature*. 2017;545:238-242.

35. Jin YR, Yoon JK. The R-spondin family of proteins: emerging regulators of Wnt signaling. *Int J Biochem Cell Biol*. 2012;44:2278-2287.

SUPPORTING INFORMATION

Additional supporting information may be found online in the Supporting Information section at the end of this article.